Proceedings of the ASME VVUQ 2022 Symposium
VVS2022
May 25-26, 2022, College Station, Texas, USA

VVS2022-86806

VALIDATION ANALYSIS OF MEDIUM-SCALE METHANOL POOL FIRE

Jared Kirsch[1,2*], Nima Fathi[2,3], Joshua Hubbard[1]

[1]Sandia National Laboratories, NM, USA
[2]University of New Mexico, NM, USA
[3] Texas A&M University, TX, USA

ABSTRACT

A 30-cm diameter methanol pool fire was modeled using Sandia National Laboratories SIERRA/Fuego turbulent reacting flow code. Large Eddy Simulation (LES) with subgrid turbulent kinetic energy closure was used as the turbulence model. Combustion was modeled and simulated using a strained laminar flamelet library approach. Radiative heat transfer was modeled using the gray-gas approximation. In this investigation, the area validation metric (AVM) is employed to examine simulation results against experimental data. Time-averaged values of temperature and axial velocity at multiple locations along the domain centerline are analyzed for two computational meshes. Two time ranges for averaging temperature and axial velocity are evaluated, and the relationship between the results and the underlying physics is mentioned. Flame height is estimated using an intermittency definition, and the effect of the threshold variable is discussed. Temperature and mixture fraction were used as threshold variables, and the sensitivity of flame height to changes in each is examined. This study aims to increase understanding of the simulation results in light of a specific validation metric, and serve as a start to further validation studies.

Keywords: Pool fire; validation; turbulent reacting flow

1. INTRODUCTION

Robust fire modeling is a challenging objective, but offers high reward as a complement to experimentation regarding fire hazards. Specifically, hydrocarbon pool fires are of interest due to the hazards which they present in scenarios from industrial facility accidents to military systems transport [1, 2]. Accurate modeling requires validation of the model against experimental data to ensure that the predictions of the model reflect real physics.

A pool fire of intermediate/moderate scale can be characterized by the formation of a diffusion flame on top of a horizontal fuel where buoyancy forces are contributing to the transport mechanism [3]. The 30 – 31-cm diameter methanol pool fire is a specific validation case of the International Association for Fire Safety Science (IAFSS) Working Group on Measurement and Computation of Fire Phenomena (MaCFP Working Group). This moderate-scale methanol pool fire has been well characterized experimentally, with several detailed studies being reported in [4-11]. The fires were characterized by measurements of velocity and temperature, fluxes of heat and mass, chemical composition, and other quantities. In particular, Weckman [4] conducted one of the earliest studies on this methanol fire at the University of Waterloo. This study provided a velocity and temperature dataset containing mean and RMS values, length scales, turbulence intensity, and correlations. In addition, the description of the experimental setup, entrainment phenomena, and other flow characteristics provided valuable background to the current study. Klassen and Gore [10] reported the radiative heat loss fraction, flame height, fuel mass burning rate, and radiative heat flux, among other quantities.

Though temperature and velocity are heavily utilized as validation parameters in pool fire studies, the complex physics involved in turbulent reacting flows allow for the examination of additional quantities. In this study, the Area Validation Metric is harnessed to compare the computational results and experimental data statistically. Quantities evaluated include the temperature, axial velocity, and flame height. All quantities are compared to experimental data, largely from Weckman, but with flame height being that reported by Klassen and Gore.

* Corresponding author

2. SIMULATION DETAILS

Sandia National Laboratories (SNL) developed a low-Mach module for simulation of turbulent reacting flow, specifically as the primary element in the ASC fire environment simulation project [12]. This module of the SIERRA code suite is known as Fuego, and represents the turbulent, buoyantly-driven incompressible flow, heat transfer, mass transfer, combustion, soot, and absorption coefficient model portion of the simulation software. Using Multiple-Program-Multiple-Data (MPMD) coupling, Fuego is coupled to Nalu for Participating Media Radiation (PMR) modeling.

Fuego has multiple options for turbulence modeling and, in this project, a Large Eddy Simulation (LES) scheme was used, with closure being provided by a subgrid-scale (SGS) kinetic energy one-equation (or K SGS) closure model. The LES methodology resolves the behavior of the larger eddies explicitly, while modeling the small eddies characterized by the subgrid scale approximately.

The difference between these divisions is characterized by length scale Δ, which, if the eddy size ≥ Δ, implies that the eddy belongs to the larger eddies that are resolved, and if the eddy is smaller than Δ, it belongs to the small eddy category which is modeled with subgrid-scale models [13,14].

LES uses spatial filtering and was chosen since it produced time-varying results which were essential for calculation of statistics necessary for comparison with experimental data.

Turbulent combustion modeling was performed in Fuego using a Strained Laminar Flamelet Model (SLFM), in which turbulent flames are treated as an ensemble of laminar diffusion flames, and nonequilibrium chemistry is included by accounting for localized fluid strain. By resolving chemical scales in the phase space of the mixture fraction instead of a 3D grid, computational efficiency is improved [12]. Chemistry is assumed to occur only in a thin layer around stoichiometry and to be quasi-steady on the scale of the flow. Thus, the chemical structure in mixture fraction space is pre-computed and the resulting table is queried during the simulation to obtain flow properties.

The pool fire geometry closely followed related experiments [4, 10]. The characteristic dimension of the pan is the diameter (30 cm), and the rim/lip height, another significant dimension, was 1 cm. Experiments showed that elevating the pan above the floor had an important effect on entrainment, and thus, the fuel surface was located 0.25 m above the bottom of the simulation domain. An overall domain height of 2.25 m and diameter of 2 m allowed for a realistic solution out to ambient conditions.

Figure 1 shows the simulation domain with boundary conditions. Mass flux was prescribed on the pool surface as 0.0151 kg/m^2-s (value from Weckman experiment). The pool temperature was set at 333 K, mixture fraction was specified as 1.0 and scalar variance was set to 0.0. The bottom of the domain and the pan surfaces were specified as constant temperature walls at 298 K. The other domain boundaries were modeled as outflow boundaries with 0 gage pressure, 0 velocity, 0 mixture fraction, and temperature being 298 K. Additional parameters are discussed in more detail in Hubbard et al. [15].

Methanol simulations were run with two mesh sizes and the results examined to determine the effect of mesh refinement on key quantities in the solution. The coarse mesh had 3,006,446 nodes and 2,363,433 cells, while the fine mesh had 6,177,500 nodes and 4,827,253 cells.

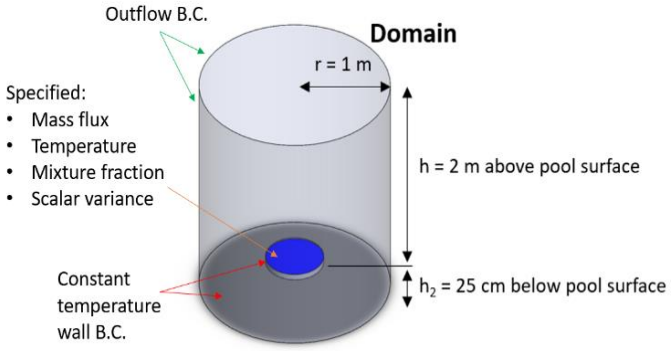

FIGURE 1: SIMULATION DOMAIN AND BOUNDARY CONDITIONS.

3. THEORY

3.1 Flame Height

Flame height is one of the most distinct visual parameters of a pool fire, and is often reported as a characteristic geometric feature [10]. Various engineering correlations exist for the prediction of flame height, and several relate the flame height to the fire diameter [16]. A common engineering correlation [17] used for estimation of mean flame height is given in the SFPE Handbook of Fire Protection Engineering (Eq. (1) below). In this relationship, L is the mean flame height in meters, D is the pan diameter in meters, and $\dot{Q} = \dot{m}_f H_c$ is the total heat release rate in kW, where $\dot{m}_f$ is the fuel mass burning rate in kg/s and H_c is the lower heat of combustion of the fuel in kJ/kg.

$$L = -1.02D + 0.235\dot{Q}^{2/5} \quad (1)$$

Because fires are unsteady flows, the spatial location of the flame tip varies with time. Thus, flame height is often taken as the height at which the intermittency is 50%, meaning that 50% of the time, the flame tip passes that spatial location. The flame tip may be defined visually or in terms of another parameter such as temperature or mixture fraction. The latter approach is taken in this study.

3.2 Area Validation Metric

Validation can be defined as the process of determining the degree to which a model is an accurate representation of the real world from the perspective of the intended uses of the model [18]. To perform a quantitative comparison between the results of the computational model and experimental results, various validation metrics can be applied. The area validation metric (AVM) is one such metric, and has been used by such authors as Oberkampf and Roy [18, 19]. This metric is defined to be the

area between the cumulative distribution function from the simulation and the empirical distribution function (EDF) which is also known as empirical cumulative distribution function from the experiment. In the case that the number of simulation samples is limited, the simulation may be represented by individual samples and an EDF for the simulation results may be used as well as for the experimental data. If the area between the EDF of the experiment and the EDF of simulation is 0, it means there is no evidence that the simulation and the experiment are in disagreement. This study uses the AVM to draw several conclusions regarding parameters from the simulation results. The difference in areas is designated as d. In the figures which present the AVM below, the colored areas are the difference between experimental and simulation cumulative values. The red area represents the positive difference (d^+) and the blue area represents the negative difference (d^-) which are evaluated for the model form uncertainty. If S is considered as the simulation mean value or the function simulation results, the model form uncertainty can be presented as $[S - F_s d^-, S + F_s d^+]$, $F_s = 1.25$, where F_s is the factor of safety [18-21].

4. RESULTS AND DISCUSSION

4.1 AVM for Temperature and Axial Velocity

Figure 2 shows a contour plot of time-averaged temperature for the fine mesh. The temperature equals the boiling point of methanol (338 K) at the pool surface. There is a relatively high temperature core region of the flame in which the energy balance involving heat from combustion and heat losses is relatively high. Outside this region, the net energy balance is lower (lower heat input and higher losses), resulting in lower temperature. This decrease in temperature continues outward from the high temperature region until ambient temperature (298 K) is reached.

Temperature and axial velocity were temporally averaged at five axial locations (z = 2, 4, 6, 8, 10 cm above the pool surface). EDFs were formed from the simulation results and University of Waterloo data. Figure 3 shows the AVM for temperature at these axial locations for both the coarse and fine meshes. For temperature, the simulation data is moderately lower than the experimental data for both meshes. The metric shows a higher area for the fine mesh, implying higher error in the simulation results. However, the AVM for axial velocity (Figure 4) shows very similar areas for both meshes, with the area for the fine mesh being slightly lower than that for the coarse mesh. Taken together, these results for the AVM indicate that refining the mesh did not substantially decrease uncertainty in the simulation results. Because this particular fire is a validation case for the International Association for Fire Safety Science (IAFSS) Working Group on Measurement and Computation of Fire Phenomena (MaCFP Working Group), several other groups have modeled it with similar meshes and reported similar results. This factored into confidence in the mesh resolution. The meshes used in this study were believed to be adequate, and were the best achievable given the computational resource constraints under which the study was conducted.

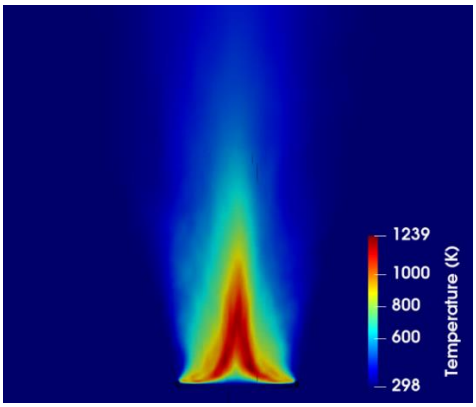

FIGURE 2: CONTOUR PLOT FOR TIME-AVERAGED TEMPERATURE.

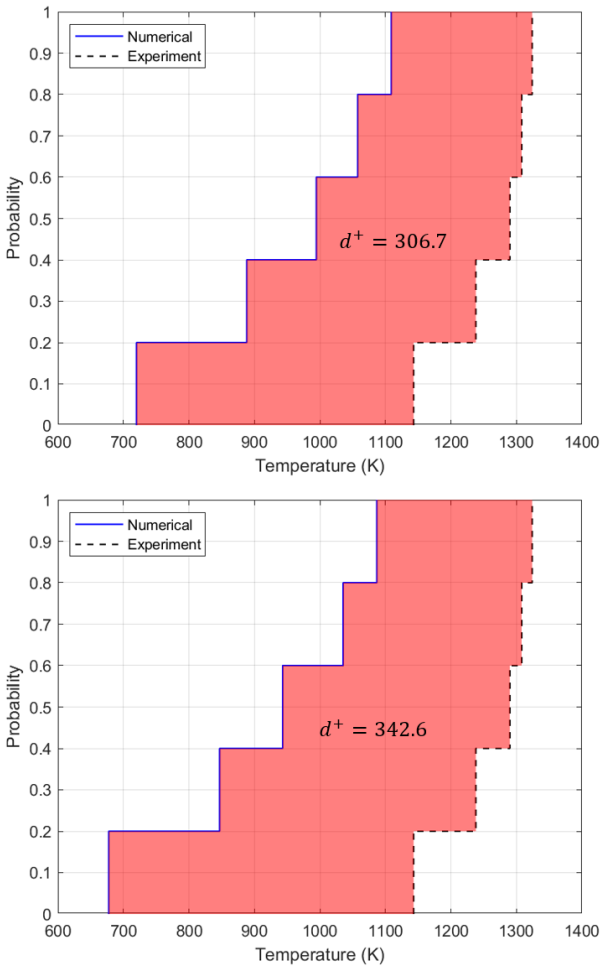

FIGURE 3: AREA VALIDATION METRIC FOR TIME-AVERAGED TEMPERATURE FOR COARSE (TOP) AND FINE (BOTTOM) MESHES.

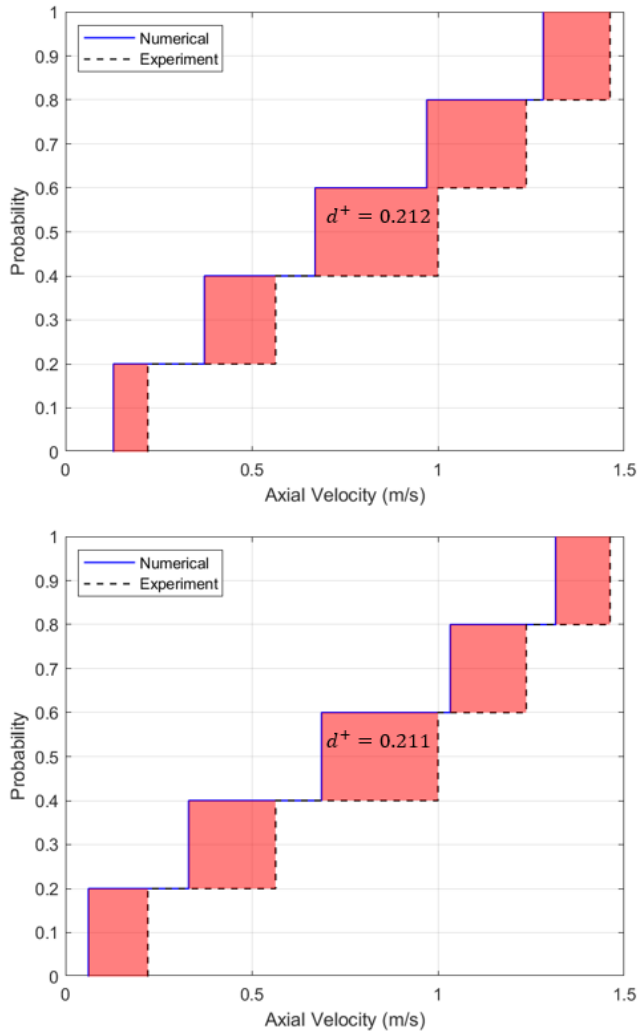

FIGURE 4: AREA VALIDATION METRIC FOR TIME-AVERAGED VELOCITY FOR COARSE (TOP) AND FINE (BOTTOM) MESHES.

The cumulative distribution function (CDF) of time series data can also be examined using a similar approach. The pool fire exhibits roughly periodic behavior, with a puffing frequency corresponding to the behavior of the large-scale eddies and entrainment of air into the plume. Thus, a sufficiently large time period must be considered for time-averaging the data in order to truly capture average physics. At the same five axial locations, time series of temperature data were plotted as cumulative distribution functions along with the single experimental result from the University of Waterloo data. A time range of 10 s, from 15 – 25 s, was used for these series and found to offer good convergence. The time series of temperature data at $z = 4$ cm on the centerline is shown in Figure 5. An interesting conclusion can be made by comparing the area to the right of the experimental value *and above the intersection with the CDF* (d_a^-) with the area to the left of the experimental value. This gives an indication of how much time was spent above the experimental value vs. below it for that spatial location. In Figure 5, then, it is seen that the temperature at $z = 4$ cm was below the experimental value for significantly more of the time range considered than above, and the simulation uncertainty at that point will reflect the fact that the temperature from the simulation was lower than the experimental value. Comparing such plots for two time ranges (17 – 18 s and 15 – 25 s) showed that the CDF was more symmetric about the experimental value for the larger time range, indicating a better description of the average physics. Comparing plots for the five axial locations gave an indication of how the time series was distributed about the experimental value at each location.

Figure 6 shows a similar plot for the axial velocity time series (15 – 25 s) at $z = 4$ cm on the centerline. In this plot, the simulation values are again seen to be lower than time-averaged experimental value for more of the time range.

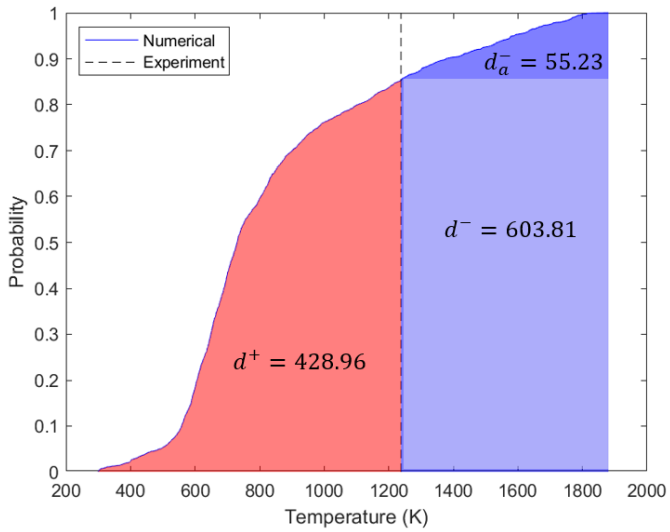

FIGURE 5: AREA VALIDATION METRIC FOR TIME SERIES OF TEMPERATURE AT Z = 4 CM.

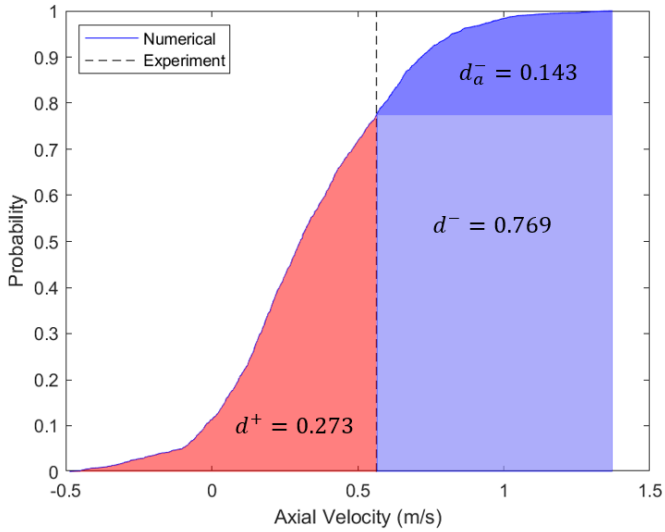

FIGURE 6: AREA VALIDATION METRIC FOR TIME SERIES OF AXIAL VELOCITY AT Z = 4 CM.

4.2 AVM for Flame Height

To compute the flame height using simulation data and the intermittency definition, a time-series of data was examined at several heights above and below the experimentally reported flame height. At each of these points, the median temperature (the temperature which is surpassed 50% of the time) at each height was compared to a threshold temperature. The median temperature was used rather than the time-averaged temperature because 1) the median is a better representation of 50% intermittency and 2) the time-average was shown to be biased higher than the median due to large-magnitude fluctuations occurring more frequently above the average than below. When the threshold temperature and median temperature at a given height were in sufficient agreement (5-10%), that height could be taken as the flame height. Besides temperature, mixture fraction was also used as a threshold variable. It was determined that 5 s of simulation data were required to calculate sufficiently accurate results.

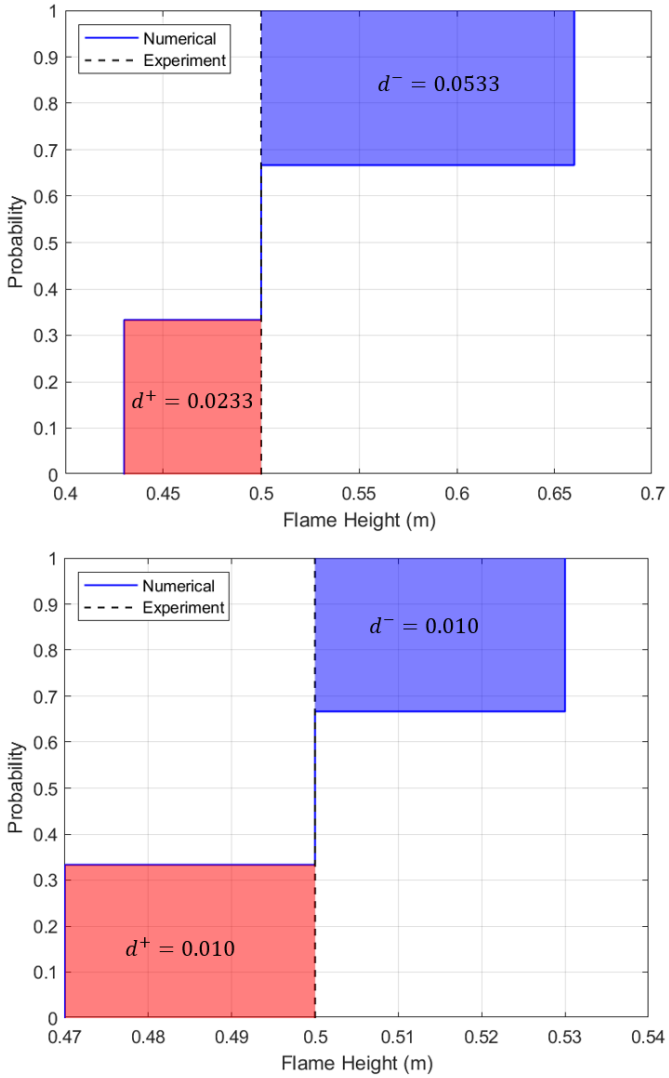

FIGURE 7: AREA VALIDATION METRIC FOR FLAME HEIGHT COMPUTED WITH TEMPERATURE (TOP) AND MIXTURE FRACTION (BOTTOM) AS THRESHOLD VARIABLES.

To examine the effect of the threshold variable used in the estimation of flame height as well as the sensitivity of each variable to variations, the threshold variables were varied by the same percent difference about the value which yielded the experimentally expected flame height. Each variable was thus increased and decreased by 15%, and the resulting flame height estimates were used in the AVM. Figure 7 shows the AVM for flame height computed using both threshold variables. Within the range examined, the flame height was found to be less sensitive to the mixture fraction and more symmetric about the experimental value. A larger range was also examined but is not shown because the same trends were exhibited, but were shown less clearly for more points.

4.3 Uncertainty Estimates from AVM

The overall application of the AVM to the simulation results and implications of the validation study are realized by computing uncertainty estimates using the AVM from the plots shown in preceding sections. Table 1 gives the high and low side uncertainty estimates for each result as a percentage of the average value, and the resulting range for each QOI, where temperature is in K, velocity in m/s, and flame height in meters.

QOI	Uncertainty (%)	Range
T, coarse mesh	[-40.19, +40.19]	[570.59, 1337.27]
T, fine mesh	[-46.64, +46.64]	[489.86, 1346.24]
U, coarse mesh	[-38.61, +38.61]	[0.421, 0.950]
U, fine mesh	[-38.41, +38.41]	[0.423, 0.949]
T, z = 4 cm	[-6.52, +50.65]	[791.75, 1275.94]
U, z = 4 cm	[-43.21, +82.49]	[0.188, 0.604]
Flame height, T	[-10.66, +4.66]	[0.447, 0.523]
Flame height, MF	[-2, +2]	[0.49, 0.51]

Table 1: UNCERTAINTIES AND ASSOCIATED INTERVALS FOR EACH QOI.

It is seen in Table 1 that the uncertainty predicted by the AVM is 38 – 47% for the temperature and axial velocity shown in Figures 3 and 4. Hubbard [15] gives a collection of plots comparing simulation and experimental data over radial and axial profiles, and states that axial velocity, for example, agrees with experimental values to within 20 – 30% in general. This is consistent with the AVM findings when the influence of the factor of safety in the AVM estimate is considered, and shows the conservative nature of the AVM for this problem. As explained by Hubbard, the difference between simulation and experimental values for these simulations is comparable to that of similar simulation studies. It is noted that for the time series data, the AVM uncertainties do not give an indication of the accuracy of the simulation value, but rather an indication of how likely the simulation value is to be larger and smaller than the experimental value, depending on the bound, for the given time interval. Lastly, the uncertainties on the flame height predictions

are below 11% for the range of threshold variables considered, which indicates that the value of the threshold variable may be varied more due to lack of prior knowledge without significantly affecting predictive accuracy. Taken together, the AVM results show that this metric may be used to estimate uncertainty for multiple dataset types and predict conservative ranges for simulation QOIs. The results indicate that the AVM gives a realistic estimate of uncertainty for time-averaged QOIs and that the simulation results generally differ from experimental data by amounts seen in related simulation studies [15].

5. CONCLUSION

The area validation metric was used to analyze results from a medium-scale methanol pool fire simulation. Time-averaged temperature and axial velocity data were analyzed at several locations for a high-level perspective. An alternative use of the AVM for analysis of time series was described. The flame height predicted with an intermittency definition was examined for two threshold variables. In general, the AVM predicted reasonable, albeit conservative uncertainties for simulation quantities. These uncertainties demonstrated model accuracy consistent with similar, recently published, studies. Model improvements and a more thorough mesh refinement study are always advantageous. However, these come at a substantial computational cost considering the broad parametric study performed by Hubbard et al. [15]. The AVM shows potential to give accurate predictions of uncertainty for time-averaged QOIs at individual spatial locations as indications of uncertainty for collections of such points. Ideally, this study would be extended to include the use of the AVM on more QOIs at more spatial locations. Its use on time series data could also be investigated further. The AVM metric may prove useful for future simulations using this code suite, including sooting flames. This study extends understanding of the simulation results as compared with experimental data and results from other simulations.

REFERENCES

[1] Ahmadi, O. et al., 2019, “Consequence analysis of large-scale pool fire in oil storage terminal based on computational fluid dynamic (CFD)”, *Process Safety and Environmental Protection* 123, pp. 379-389.

[2] Lopez, A. R., Gritzo, L. A., Sherman, M. P., 1998, “Risk Assessment Compatible Fire Models (RACFMs)”, Report No. SAND97-1562, Sandia National Laboratories.

[3] Joulain, Pierre. "The behavior of pool fires: state of the art and new insights." In *Symposium (International) on Combustion*, vol. 27, no. 2, pp. 2691-2706. Elsevier, 1998.

[4] Weckman, E. J., Strong, A. B., 1996, “Experimental Investigation of the Turbulence Structure of Medium-Scale Methanol Pool Fires”, *Combust. Flame* 105, pp. 245-266.

[5] Buch, R., Hamins, A., Konishi, K., Mattingly, D., Kashiwagi, T., 1997, “Radiative Emission Fraction of Pool Fires Burning Silicone Fluids”, *Combust. Flame* 108, pp. 118-126.

[6] Falkenstein-Smith, R., Sung, K., Chen, J., Hamins, A., 2020, “Chemical Structure of Medium-Scale Liquid Pool Fires”, *Fire Safety Journal* 120, 103099.

[7] Falkesntein-Smith, R., Sung, K., Chen, J., Harris, K., Hamins, A., 2020, “The Structure of Medium-Scale Pool Fires”, NIST Technical Note 2082, National Institute of Standards and Technology.

[8] Hamins, A., Lock, A., 2016, “The Structure of a Moderate-Scale Methanol Pool Fire”, NIST Technical Note 1928, National Institute of Standards and Technology.

[9] Kim, S.C., Lee, K.Y., Hamins, A., 2019, “Energy Balance in Medium-Scale Methanol, Ethanol, and Acetone Pool Fires”, *Fire Safety Journal* 107, pp. 44-53.

[10] Klassen, M., Gore, J. P., 1994, “Structure and Radiation Properties of Pool Fires”, NIST-GCR-94-651, National Institute of Standards and Technology.

[11] Wang, Z., Tam, W. C., Chen, J., Lee, K.Y., Hamins, A., 2019, “Thin Filament Pyrometry Field Measurements in a Medium-Scale Pool Fire”, *Fire Technology* 56, pp. 837-861.

[12] Black, A., Aro, C., Brown, A., Burns, S., et al., 2021, “SIERRA Low Mach Module: Fuego Theory Manual – Version 5.0”, Report No. SAND2021-3929, Sandia National Laboratories.

[13] Aleyasin, S. S., Fathi, N, Tachie, M. F., Peter Vorobieff, P., Koupriyanov, M., 2017, “Experimental-numerical analysis of turbulent incompressible isothermal jets”, *Fluids Engineering Division Summer Meeting*, vol. 58066, p. V01CT23A015, American Society of Mechanical Engineers.

[14] Rodriguez, S. B., Fathi, N., “Applied Computational Fluid Dynamics and Turbulence Modeling”, No. SAND2017-13577B. Sandia National Lab.(SNL-NM), Albuquerque, NM (United States), 2017.

[15] Hubbard, J. A., Hansen, M. A., Kirsch, J. R., Hewson, J. C., Domino, S. P., Submitted for review September 2021, “Medium Scale Methanol Pool Fire Model Performance Validation”, *ASME Journal of Heat Transfer*.

[16] Iqbal, N., Salley, M. H., 2004, “Fire Dynamics Tools (FDT): Quantitative Fire Hazard Analysis Methods for the U.S. Nuclear Regulatory Commission Fire Protection Inspection Program”, Report No. NUREG-1805, U.S. Nuclear Regulatory Commission.

[17] Heskestad, G., 2016, “Fire Plumes, Flame Height, and Air Entrainment, SFPE Handbook of Fire Protection Engineering”, Springer.

[18] Roy, C. J., Voyles, I., 2013, “Assessment of Model Validation Approaches using the Method of Manufactured Universes”, *ASME Verification and Validation Symposium.*

[19] Oberkampf, W. L., Roy, C. J., 2010, “Verification and Validation in Scientific Computing”, Cambridge University Press.

[20] Shen, Yu-Lin, Fathi, N., 2022, “Numerical Study of Elastic-Plastic Behavior of Pore-Containing Materials: Effects of Pore Arrangement”, *International Journal of Theoretical and Applied Multiscale Mechanics*, vol. 3, no. 4, pp. 262-286.

[21] Fathi, N., Aleyasin, S. S., Wayne, P, and Vorobieff. P., 2017, “Computational Assessment of Double-Inlet Collector in Solar Chimney Power Plant Systems”, *Fluids Engineering Division Summer Meeting*, vol. 58059, p. V01BT08A006, American Society of Mechanical Engineers.